

## Compressed sensing and Sequential Monte Carlo for solar hard X-ray imaging

A. M. MASSONE<sup>(1)(2)</sup>, F. SCIACCHITANO<sup>(1)</sup>, M. PIANA<sup>(1)(2)</sup> and A. SORRENTINO<sup>(1)(2)</sup>

<sup>(1)</sup> *Dipartimento di Matematica, Università di Genova, Genova, Italy*

<sup>(2)</sup> *CNR - SPIN, Genova, Italy*

**Summary.** — We describe two inversion methods for the reconstruction of hard X-ray solar images. The methods are tested against experimental visibilities recorded by the *Reuven Ramaty High Energy Solar Spectroscopic Imager (RHESSI)* and synthetic visibilities based on the design of the *Spectrometer/Telescope for Imaging X-rays (STIX)*.

### 1. – Introduction

The NASA *Reuven Ramaty High Energy Solar Spectroscopic Imager (RHESSI)* [8] and the ESA *Spectrometer/Telescope for Imaging X-rays (STIX)* [3] are two space telescopes for imaging hard X-rays that rely on rather similar imaging technologies. *RHESSI* has been decommissioned on August 16 2018 after more than 16 years of successful operations, while *STIX* is going to fly in the next two years. Both hardware allow the modulation of the X-ray flux coming from the Sun, providing as a result sparse samples of its Fourier transform, named visibilities, picked up at specific  $(u, v)$  points of the Fourier plane. Therefore, for both *RHESSI* and *STIX*, image reconstruction is needed to determine the actual spatial photon flux distribution from the few Fourier components acquired by the hard X-ray collimators [1] [2] [5] [7] [9] [10]. In Section 2 of this paper we briefly overview a reconstruction method based on compressed sensing [6]. In Section 3 we provide more insights on a Monte Carlo method for the Bayesian estimation of several imaging parameters [11] [12]. Our conclusions are offered in Section 4.

### 2. – Compressed sensing for hard X-ray image reconstruction

Figure 1 shows how *RHESSI* and *STIX* grids sample the  $(u, v)$  frequency domain. From this design, it follows that the mathematical model for data formation in the framework of these two instruments is, in a matrix form:

$$(1) \quad HFx = V ,$$

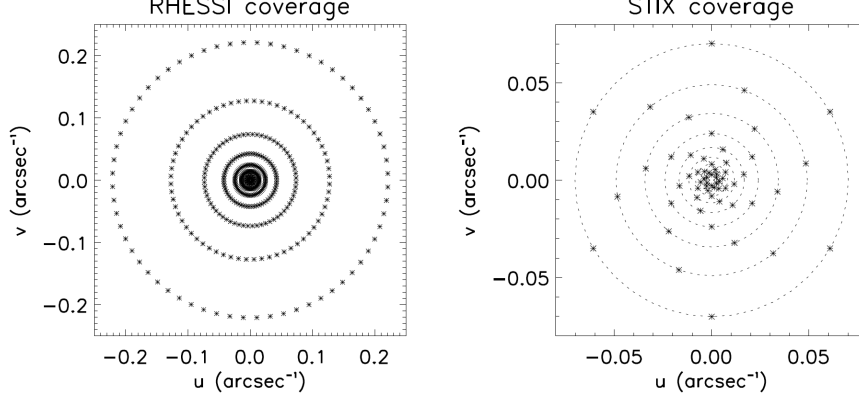


Fig. 1. – Sampling of the visibility  $(u, v)$  plane performed by *RHESSI* (left panel) and *STIX* (right panel), respectively.

where  $x$  is the photon flux image to reconstruct,  $V$  are the experimental visibilities,  $F$  is the discretized Fourier transform,  $H$  is a mask that realizes the sampling in the  $(u, v)$  plane. The reconstruction of  $x$  from  $V$  is an ill-posed problem and therefore regularization is required to mitigate the numerical instabilities induced by the observation noise. A possible approach is to apply an  $l_1$  penalty term in some transformation domain. This can be realized by solving the minimum problem [6]

$$(2) \quad \hat{x} = \min_x \{ \|HFx - V\|_2^2 + \lambda \|Wx\|_1 \} ,$$

where the regularization term  $\|Wx\|_1$  is designed to penalize reconstructions that would not exhibit the sparsity property with respect to the Finite Isotropic Wavelet Transform [6]. Figure 2 compares the reconstructions provided by this compressed sensing algorithm to the ones obtained by using other four visibility-based imaging methods currently implemented in the *RHESSI* pipeline [5] [7] [9].

### 3. – Sequential Monte Carlo for hard X-ray image reconstruction

Sequential Monte Carlo (SMC) samplers are computational methods aiming at sampling target distributions of interest, and are often applied to sample the posterior distribution  $p(x|y)$  as given by Bayes' theorem

$$(3) \quad p(x|y) = \frac{p(y|x)p(x)}{p(y)} ,$$

where  $x$  is the unknown,  $y$  is the observation,  $p(x)$  is the prior probability encoding all *a priori* information,  $p(y|x)$  is the likelihood encoding the image formation model (1) and the noise model, and the marginal likelihood  $p(y)$  is a normalization factor. In the case of *RHESSI* and *STIX* imaging,  $x$  is the image to reconstruct and  $y$  denotes the set of recorded visibilities. We modeled  $x$  as  $x(N, T_{1:N}, \Theta_{1:N})$  where  $N$  is the number of

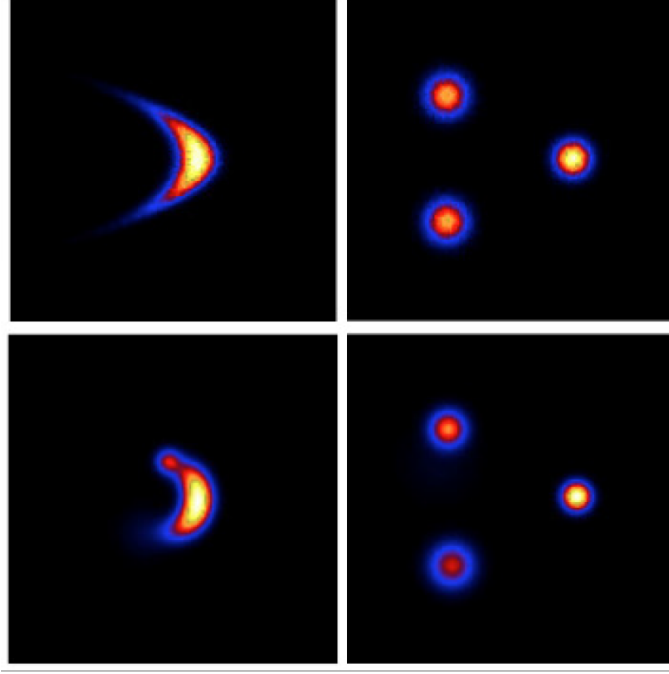


Fig. 2. – Image reconstructions from *RHESSI* visibilities provided, from left to right, by a Back-Projection algorithm, CLEAN, an interpolation/extrapolation method, a compressed sensing method based on exploiting an image catalogue, and by our wavelet-based compressed sensing method. The reconstructions refer to the May 13, 2013 event in the time interval 02:04:16-02:04:48 UT and energy range 6-12 keV. *RHESSI* visibilities recorded by detectors from 3 to 9 have been used in all cases.

sources in the image,  $T_{1:N} = (T_1, \dots, T_N)$  represents the source types (Gaussian, elliptical, loop-like) and  $\Theta_{1:N} = (\theta_1, \dots, \theta_N)$  contains the parameters characterizing each source. We chose a prior distribution factorized as the product of a Poisson distribution for  $N$ , uniform distributions for the source types and uniform distributions for the source parameters [11] [12]. Sequential Monte Carlo [4] computes the posterior distribution iteratively, by constructing a sequence of converging approximate distributions. Once the posterior is determined, it can be used to compute the solution image and all image parameters. Figures 3 and 4 show results provided by this approach using simulated *STIX* visibilities and experimental *RHESSI* visibilities, respectively.

#### 4. – Conclusions

This paper shows the performances of two image reconstruction methods formulated for hard X-ray solar visibilities. The implementation of the corresponding tools within *Solar SoftWare* (*SSW*) is under construction.

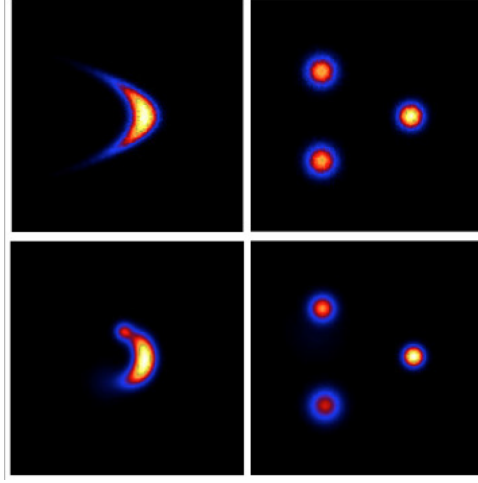


Fig. 3. – Reconstructions of two simulated configurations estimated by the SMC algorithm using synthetic *STIX* visibilities corresponding to a realistic signal-to-noise ratio. Top row: ground truth; bottom row: SMC reconstructions.

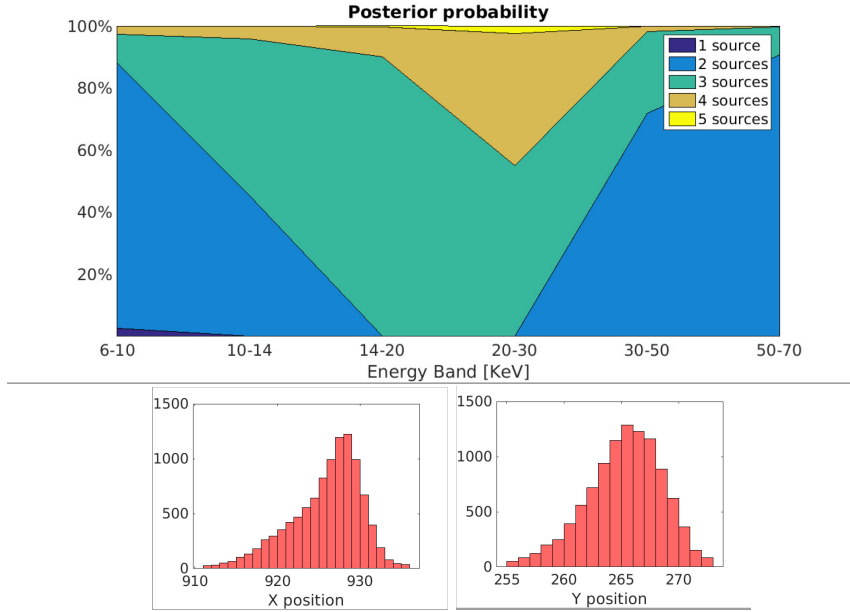


Fig. 4. – Parameters estimation provided by SMC in the case of the February 20, 2002 *RHESSI* visibilities. Top panel: posterior probabilities for the number of sources at different energy channels. Bottom panel: histograms of the  $x$  and  $y$  position of the loop-top source detected with high probability at the 20 – 30 keV channel.

## REFERENCES

- [1] ASCHWANDEN M.J., BROWN J.C. and KONTAR E.P., *Sol. Phys.*, **210** (383) 2002.
- [2] BENVENUTO F., SCHWARTZ R., PIANA M. and MASSONE A.M., *Astron. Astrophys.*, **555** (A61) 2013.
- [3] BENZ A.O. ET AL, *The Spectrometer Telescope for Imaging X-rays on board the Solar Orbiter mission*, in *Space Telescopes and Instrumentation 2012: Ultraviolet to Gamma Ray*, edited by INTERNATIONAL SOCIETY FOR OPTICS AND PHOTONICS 2012, p. 84433L.
- [4] DEL MORAL P., DOUCET A. and JASRA A., *J. R. Stat. Soc. B*, **68** (411) 2006.
- [5] DENNIS B.R. and PERNAK R.L., *Astrophys. J.*, **698** (2131) 2009.
- [6] DUVAL POO M., PIANA M. and MASSONE A.M., *Astron. Astrophys.*, **615** (A59) 2018.
- [7] FELIX S., BOLZERN R. and BATTAGLIA M., *Astrophys. J.*, **849** (10) 2017.
- [8] LIN R.P. ET AL, *Sol. Phys.*, **210** (3) 2002.
- [9] MASSONE A.M., EMSLIE A.G., HURFORD G.J., PRATO M., KONTAR E.P. and PIANA M., *Astrophys. J.*, **703** (2004) 2009
- [10] METCALF T.R., HUDSON H.S., KOSUGI T., PUETTER R.C. and PINA R.K., *Astrophys. J.*, **466** (585) 1996.
- [11] SCIACCHITANO F., LUGARO S. and SORRENTINO A., *SIAM J. Imag. Sci.*, *accepted*, (arXiv preprint:1807.11287) .
- [12] SCIACCHITANO F., SORRENTINO A., EMSLIE A.G., MASSONE A.M. and PIANA M., *Astrophys. J.*, **862** (68) 2018.